

# A Study of Epitaxial Growth of GaN And InGaN/GaN Heterostructure on A-Plane Sapphire Substrates

Snehil<sup>1\*</sup>, Dr. Alope Verma<sup>2</sup>

<sup>1</sup> PhD Student, Kalinga University, Raipur

<sup>2</sup> PhD Guide, Kalinga University, Raipur

**Abstract** - Group-III nitride-based semiconductors have shown promising promise as the foundation for a new generation of optoelectronic, high-temperature, and high-power microelectronic devices. Due to the high cost of GaN templates and the difficulty of growing GaN single crystals, this material is typically grown heteroepitaxially on incompatible substrates such as Al<sub>2</sub>O<sub>3</sub>, SiC, Si, etc. Even if the crystal quality of epitaxial layers has vastly improved thanks to developments in growth technology, there is still an issue with the considerable discrepancy in lattice constants and thermal expansion coefficients between the epitaxial layer and the substrate. C-plane (0001) sapphire has been the primary focus of research on substrates that can support the growth of high-quality epitaxial GaN films. The substantial mismatch between the lattice (14%) and thermal expansion coefficient (56%), which has hindered the nucleation and growth of epitaxial GaN, has prompted the development of a number of strategies for optimizing these processes. High densities of different crystallographic defects, like dislocations and domain borders, etc., impede the growth of GaN on c-plane sapphire. In contrast, a-plane sapphire substrates have been reported in the literature as a replacement for c-plane sapphire substrates due to the smaller lattice mismatches between [0002] GaN parallel to [1120] sapphire and [1100] GaN parallel to [1100] sapphire. A decrease in lattice mismatch will allow for the formation of GaN with higher crystalline quality, fewer flaws, and hence superior devices. Growth of GaN films on a-plane sapphire with early nitridation and low temperature GaN buffer layers results in smooth surface morphology. The influence of trap states, centers for radiative and non-radiative recombination in the material, must be taken into account in addition to smooth surface morphology and crystalline quality, both of which are prerequisites for device competent semiconductor material. The impact of GaN and AlN buffer layers on GaN development on a-plane sapphire has also been investigated.

**Keywords** - Epitaxial Growth, INGAN/GAN Heterostructure, semiconductors, crystalline quality, GaN development

-----X-----

## INTRODUCTION

InGaN/AlGaIn multiple quantum well LEDs produced on a-plane and c-plane sapphire substrates have only been compared by a small number of research organizations. LEDs grown on a-plane sapphire substrates were shown to have better crystallographic and optoelectronic qualities than LEDs grown on c-plane sapphire substrates under the same conditions. These properties included narrower x-ray diffraction lines, lower pit densities, and a lower ideality factor. GaN grown on an a-plane sapphire substrate, however, has not been thoroughly investigated from a device fabrication standpoint. In order to gain a thorough understanding of the high quality epitaxially produced GaN film, it is crucial to study its structural and optical properties while it is grown on an a-plane sapphire substrate. We have shown that an epitaxially grown GaN layer on an a-plane sapphire substrate can

have a high crystalline quality, and we have investigated its structural and optical properties at length. The effect of flaws on device performance should be thought about from the standpoint of device manufacture as well. Therefore, I-V and Transient Spectroscopy are used to investigate and incorporate the created defect states and associated dynamics. Furthermore, InGaN based device structure have lately emerged as the primary stream of Nitride solar cell structure, taking into account the potential application of whole solar spectrum photovoltaic applications and the appropriateness to the engineering of bandgap energies. Due to the substantial lattice mismatch (11%) between InN and GaN and the relatively high-vapor pressure of InN compared to the vapor pressure of GaN, a solid-phase miscibility gap has been discovered. Since this is the case, just a small amount of indium is added to the InGaN alloy. There are various

obstacles to overcome when trying to control phase separation and defect density in InGaN development, leading to subpar device performance. Growing InGaN materials with a high indium content and crystalline quality is the current problem in manufacturing high efficiency III-nitride solar cells. As a result, we have conducted more research into the growth of InGaN/GaN heterostructures on an a-plane sapphire substrate, focusing on their structural and optical features. InGaN grown on an a-plane sapphire substrate has not been the subject of any in-depth research up until now. In this work, we show that a high-Indium-content (41%) InGaN/GaN heterostructure can be grown on a (112,0) sapphire substrate with good crystalline quality, shedding light on the structural quality of In-rich InGaN/GaN based heterostructures on a-plane sapphire substrate.

## MATERIALS AND METHODS

### 1 Synthesis of GaN and GaN/InGaN heterostructure

For the GaN growth on the (112,0) sapphire substrate, we used a RIBER Compact 21 PAMBE system with typical Riber PBN effusion cells and an RF - plasma source to supply the active nitrogen ( $N^*$ ) species. Chemical pre-cleaning was performed on the a-plane sapphire substrate using the normal cleaning process, and then out-gassing was performed in the buffer chamber at 600 °C. GaN on an a-plane sapphire substrate (S1) and an InGaN/GaN heterostructure on an a-plane sapphire substrate (S2) are the two samples that have been generated. The substrate temperature throughout the nitridation process was just 450 degrees Celsius. At 530 degrees Celsius, Ga-rich conditions were used to deposit an LT-GaN buffer layer. At 735 degrees Celsius with an rf plasma power of 500 W, the epitaxial GaN layer grew at a rate of 3 nm/min (Ga beam equivalent pressure [BEP] of  $9E-7$  Torr). The second sample S2 uses the identical GaN growth conditions to develop an InGaN/GaN heterostructure, with the InGaN epitaxial layer grown at 610 °C and an Indium (In) BEP of  $2.0E-7$  Torr while maintaining a constant Ga flux. Cross-sectional schematic of GaN and InGaN/GaN heterostructure formed on a-plane sapphire substrate using the identical GaN film growth process for InGaN/GaN heterostructure creation is shown in Fig. 4.1. As a first step, we have used a wide range of characterisation techniques to assess the generated GaN film's quality. Below, we will go into greater depth about the specific characterisation methods employed in this chapter.

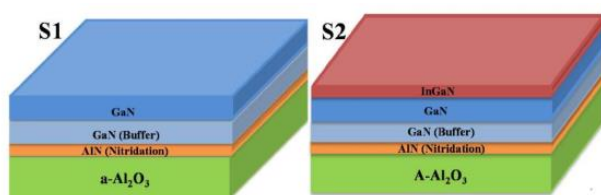


**Figure 1: Schematic diagram of individually stacked layers on a-plane sapphire substrate for samples S1 and S2**

### 2 Characterizations Tools

RHEED used a STAIB electron gun to keep an eye on things locally, while an optical pyrometer (error value 5 °C) calibrated with a thermocouple tracked the growing temperature. HRXRD at a scan rate of 0.05°/sec and slit width of 0.1mm was used to analyze the growth structure and crystalline nature of GaN film, while FESEM was used to evaluate the morphological properties of produced GaN films. TOF-SIMS was used to verify the elemental composition and InGaN/GaN heterostructure thickness. Moreover, PL and Raman spectroscopy have been utilized to delve deeper into the grown film's optical characteristics. I-V measurements were used to examine the electrical characteristics of the grown film. The samples were cleaned according to industry standards before being loaded into an evaporation chamber to deposit metal contacts. Each sample was washed with acetone, methanol, and isopropanol, in that order, to get rid of any organic, inorganic, or physical contaminants like dust or excess moisture. Next, compressed nitrogen was used to dry the wafers. Contacts were fabricated using PVD-deposited gold. A Micra oscillator, Coherent Legend amplifier, TOPAS optical parametric amplifier, and spectroscopy equipment have been used to accomplish femtosecond transient absorption spectroscopy (Helios, Ultrafast Systems). The amplifier's output is divided into two channels, each of which receives half of the 4 mJ (1 KHz) of power with a 35 fs pulse width and an 800 nm center wavelength. This splits the energy into two pieces, with 1.8 mJ going to the OPA and 0.5 mJ going to the spectrometer via a delay stage of 0-8 ns. In most cases, TOPAS reduces the pulse width to around 70 fs. This spectrometer's broad band white light is produced by passing the spitted beam through a sapphire cylindrical crystal that can produce a probe pulse in the 450-850 nm range. The OPA output was narrowed down to a steady 320 nm for use as the pump beam, and the fluence was set to 40 J/cm<sup>2</sup>. Surface Xplorer analysis software is used to perform the fitting of the data.

### RESULTS AND DISCUSSION

Figure 2 is a crystallographic cross-sectional representation of the contact between GaN and an a-plane sapphire substrate (a). Our experimental RHEED data, reported below, show that the epitaxial orientation relationship of (0001) GaN/(1120) sapphire is implied by GaN development on a-planar sapphire. Sapphire with a N-atom monolayer on top, as shown in Fig. 2 (a). Oxygen atoms are known to serve as surface terminations for the sapphire lattice. Since the creation of a Ga-O layer at the interface due to the presence of oxygen species can impede the epitaxy of GaN, a monolayer of strained AlN is grown by exposing a-plane

sapphire to nitrogen plasma, which removes all the oxygen atoms from the surface and replaces them with nitrogen atoms. As a result, GaN may be grown more easily on a substrate with a more favorable chemical composition. Fig. 2 depicts the RHEED pattern seen in GaN along the (1120) and (1100) zone axes (b, c).

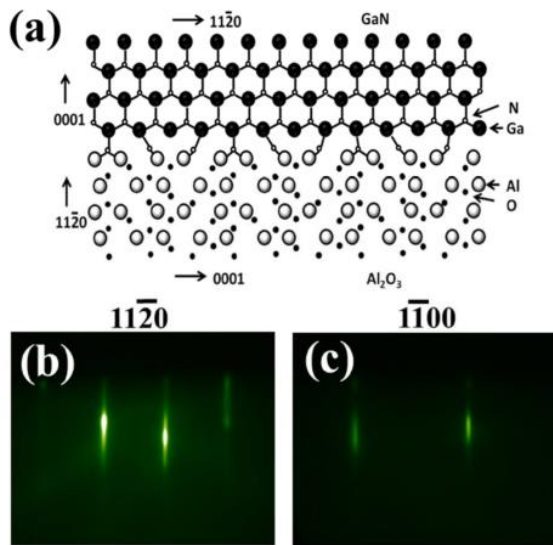


**Figure 2: (a) A crystallographic model of cross-sectional view of the GaN and a-plane sapphire interface. (b, c) Real time RHEED patterns observed along the 1120) and 1110) zone axis for GaN**

GaN film's typical 1x1 reconstructed RHEED pattern features crisp, streaky peaks and valleys. Two-dimensional (2D) growth of GaN epitaxial film with high crystalline quality may be seen in the kikuchi diffraction pattern along the (112,0) direction. The inter-planar spacing of the planes responsible for the pattern was estimated by using the camera length of the diffraction system. These results corroborated the (0001) GaN/(1120) sapphire epitaxial orientation relationship observed in GaN grown on a-plane sapphire. As a result, an epitaxial GaN layer with a wurtzite structure and high crystalline quality is developed along the c-direction on an a-plane sapphire substrate. Using FESEM, we analyzed the surface morphology of the formed GaN sheet. The GaN film on an a-plane sapphire substrate is shown in a high-resolution FESEM image in Fig. 3 (a). The film's surface was covered in continuous, irregularly sized hexagonal-shaped pits. To further appreciate the pit's shape and size, a magnified section of the FESEM picture is shown in inset Fig. 3 (a). Hexagonal pits range in size from 30 nm to 70 nm on average, and the density of these defects was determined to be 6.7E8 cm<sup>2</sup>. These craters are GaN V-defects. Different sized V-defects on the surface are caused by threading dislocations (TD) with varying core energies. Because of strain relaxation between the GaN film and the substrate, V-pits may occur. Hexagonal pits mediated by V-defects are depicted schematically in Fig. 3. (b). These V faults are open, inverted pyramids with (1011) and (1101) as the adjacent hexagonal side walls [20].

Researchers have found that increased strain energy is the root cause of V-defect generation in heteroepitaxy, and that a TD is invariably present at the base of the defect. Carrier recombination and the size of lateral V-defects were found to be correlated in a recent study by Kim et al. Non-radiative recombination domains are likely to increase when the lateral size of V-pits is reduced, as this causes carriers to diffuse laterally. Accordingly, we argue that the high non-radiative recombination of carriers in the GaN film produced on a-plane sapphire may be caused by the short lateral size of the V-pits (30-70 nm). The accompanying section delves deeply into the carrier dynamics associated with the presence of defect states and their recombination (transient spectroscopy analysis). A FESEM picture of GaN/a-sapphire cross section is shown in Fig. 3 (c).

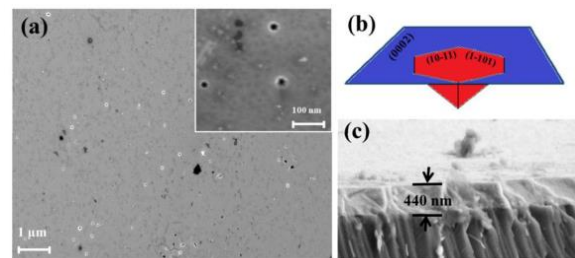


**Figure 3: (a) FESEM image of GaN film grown on a-plane sapphire substrate (b) schematic representation of hexagonal pits on the GaN surface (c) cross sectional FESEM image of GaN/a-sapphire**

The thickness of GaN was measured to be 440 nm, and a strong heterostructure interface was spotted. HRXRD investigation has shed light on the grown film's crystalline quality and provided a deeper structural examination. A 2-scan of a GaN layer produced on an a-plane sapphire substrate is displayed in Fig. 4 (a). Diffraction in the (0002) and (0004) planes of GaN are responsible for the 34.67° and 72.95° peak positions of the 2-theta mode, respectively. The lattice relaxation of the GaN film produced on a less lattice mismatched (2% along c-direction) a-plane sapphire substrate may explain why the (0002) plane diffraction angle of heteroepitaxial GaN was so near to that of strain-free bulk GaN (34.57°). In addition, the a-sapphire substrate exhibits two strong peaks at 2-theta positions of 37.9° and 80.85°, which are respectively attributed to the (1120) and (2240) diffraction planes. Highly crystalline GaN film produced along the c-direction epitaxially on an a-plane sapphire substrate is depicted by the presence of first and second order x-ray diffractions in the 2 theta-omega scan. Bragg's law is used directly to get GaN's lattice constant along its development direction (the c-axis). Lattice constant c for GaN layer was determined to be 0.5178 nm. Since the c value was decreased by 0.15% from the strain-free GaN (c=0.5185 nm) film, it can be concluded that a compressive strain is present in the hetero-epitaxially produced GaN film

on a-sapphire. By analyzing the strain, we find that an a-plane sapphire substrate with reduced lattice misfit results in the best conditions for growing a strain-relaxed heteroepitaxial GaN layer. In addition, high-resolution X-ray diffraction (HRXRD) analysis has been used to learn about the GaN epitaxial layer's crystalline quality and dislocation densities. The FWHM of GaN film is 9.83 and 28.15 arcmin in the symmetric (0002) and asymmetric (1012) planes of diffraction, respectively, as shown in Fig. 4 (b). It has been observed, however, that a thick (12 μm) GaN layer produced on a-plane sapphire by HVPE has a reduced FWHM value of symmetric scan (4 arcmin). The screw or mixed threading TD densities have been evaluated using the FWHM of the (0002) peak, and the edge TD densities have been calculated using the FWHM of the (10-12) peak. Densities of screw and mixed dislocations were determined to be 3.3 E8 cm<sup>-2</sup> in the (0002) plane of reflection, whereas densities of edge dislocations were determined to be 7.0 E9 cm<sup>-2</sup> in the (1012) plane. In other words, V-pits in a GaN film produced on an a-plane sapphire substrate are due to these TDs. A high TDs value is also indicative of the presence of non-radiative recombination centers.

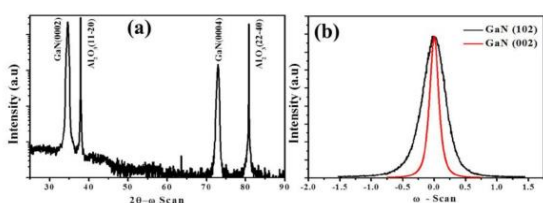


**Figure 4: (a) HRXRD 2θ- ω scan of GaN film grown on a-plane sapphire (b) ω scan spectra from the symmetric (0002) and asymmetric (10-12) plane of diffraction of GaN film**

Heteroepitaxial growth of the GaN layer on a-plane sapphire causes stresses due to the dissimilar lattice constants of the film and the substrate. Raman spectroscopy is used to analyze the stress that has built up in a grown GaN layer.

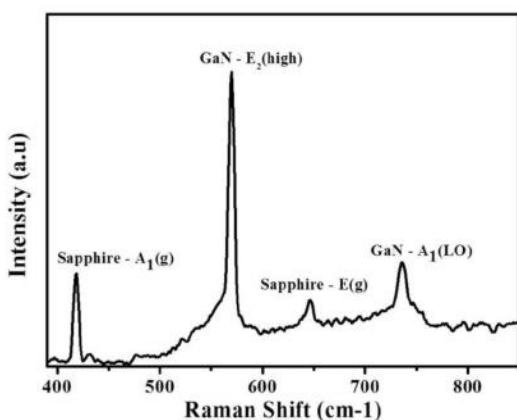


**Figure 5: RT - Raman spectra of GaN films grown on a-plane sapphire.**

The laser light is incident along the normal direction of the formed GaN film, and the RT-Raman spectrum is

acquired in a back-scattering arrangement (Fig. 5). At RT, GaN exclusively exhibits the E2 (High) and A1 (LO) phonon modes (Fig. 5). The stress/strain in a growing film is measured by measuring the frequency shift in the E2 (High) phonon mode. The E2 (high) phonon mode peak observed in this investigation for the GaN film was located at 569.8 cm<sup>-1</sup>, and as a result, this mode is the one we focus on most. The E2 (high) mode should be detectable at 567.6 cm<sup>-1</sup> in stress-free GaN material. Since the GaN film showed a blue shift of 2.2 cm<sup>-1</sup>, we can conclude that the stress in the formed film is compressive. The peaks at 735, 646, and 418 cm<sup>-1</sup> are associated with the A1(LO) phonon mode of GaN, the E(g) phonon mode of sapphire, and the A1(g) phonon mode of sapphire, respectively. For further stress quantification, a linear relationship between the E2 (high) Raman shift, and the biaxial stress, can be assumed.

### CONCLUSION

The transient spectroscopic investigation further demonstrates that these mid-gap defect states are mostly responsible from a non-radiative decay mechanism. The InGaN/GaN heterostructure produced on an a-plane sapphire substrate was also analyzed for its structural and optical properties. The smooth surface morphology and single crystalline TD density of GaN (estimated to be 4.76 E9 cm<sup>-2</sup>) of the InGaN and GaN layers in the developed heterostructure were shown. The NBE emission of InGaN was detected by PL measurements to be 1.9 eV, which agrees with the band gap determined using Vegard's law (1.88 eV; corroborated by HRXRD findings). To sum up, a high-quality crystalline InGaN/GaN heterostructure on a sapphire substrate was successfully grown, revealing new information about the structural quality of In-rich InGaN/GaN-based heterostructures necessary for high-performance optoelectronic devices. The difficulties of III-nitride epitaxial growth on a severely mismatched silicon substrate in terms of lattice and thermal expansion are then discussed. Films and structures based on GaN, AlN, and InN were explained, along with their optimization and systematic epitaxial development on a silicon substrate. Multiple structural, morphological, and optical characterizations are performed on MBE produced heterostructures, including AlN/Si(111), GaN/AlN(111), and InN(111). They demonstrate that epitaxial layers of a single crystal can be formed on silicon. Research into the structural and optical features of epitaxially grown GaN films, beginning with the impact of AlN buffer layer growth conditions, reveals that GaN films produced at high temperature in an AlN buffer layer have extremely single crystalline nature. Nevertheless, PL research confirms that DAP-related optical defects predominate in this GaN material. The second study looked at how the thickness of the epitaxial layer affected the GaN's structural, morphological, and optical properties and found that the thicker the film, the better the qualities were. Later, it was shown that epitaxial InN may grow on a Si (111) substrate at

high temperatures, leading to the development of single-crystalline micro-islands with a (10-11) orientation. As a result, a thorough comprehension of how to optimize the growth of different III-Nitride structures on Si (111) substrates has been attained.

## REFERENCES

1. M. K. Kelly, O. Ambacher, R. Dimitrov, R. Handschuh, and M. Stutzmann, "Optical process for liftoff of group III-nitride films," *Phys. Status Solidi A* 159, R3–R4 (1997).
2. M. K. Kelly, R. P. Vaudo, V. M. Phanse, L. Görgens, O. Ambacher, and M. Stutzmann, "Large free-standing GaN substrates by hydride vapor phase epitaxy and laser-induced liftoff," *Jpn. J. Appl. Phys.* 38, L217–L219 (1999).
3. W. S. Wong, T. Sands, and N. W. Cheung, "Damage-free separation of GaN thin films from sapphire substrates," *Appl. Phys. Lett.* 72, 599–601 (1998).
4. W. S. Wong, T. Sands, N. W. Cheung, M. Kneissl, D. P. Bour, P. Mei, L. T. Romano, and N. M. Johnson, "Fabrication of thin-film InGaN lightemitting diode membranes by laser lift-off," *Appl. Phys. Lett.* 75, 1360–1362 (1999).
5. T. Akane, K. Sugioka, and K. Midorikawa, "High-speed etching of hexagonal GaN by laser ablation and successive chemical treatment," *Appl. Phys. A* 69, S309–S313 (1999).
6. K. Ozono, M. Obara, A. Usui, and H. Sunakawa, "High-speed ablation etching of GaN semiconductor using femtosecond laser," *Opt. Commun.* 189, 103–106 (2001).
7. G. F. B. Almeida, L. K. Nolasco, G. R. Barbosa, A. Schneider, A. Jaros, I. Manglano Clavero, C. Margenfeld, A. Waag, T. Voss, and C. R. Mendonça, "Incubation effect during laser micromachining of GaN films with femtosecond pulses," *J. Mater. Sci.: Mater. Electron.* 30, 16821–16826 (2019).
8. L. Wei-Min, Z. Rong-Yi, Q. Shi-Xiong, Y. Shu, and Z. Guo-Yi, "Ablation of GaN using a femtosecond laser," *Chin. Phys. Lett.* 19, 1711–1713 (2002).
9. C.-F. Chu, F.-I. Lai, J.-T. Chu, C.-C. Yu, C.-F. Lin, H.-C. Kuo, and S. C. Wang, "Study of GaN light-emitting diodes fabricated by laser lift-off technique," *J. Appl. Phys.* 95, 3916–3922 (2004).
10. X. J. Su, K. Xu, Y. Xu, G. Q. Ren, J. C. Zhang, J. F. Wang, and H. Yang, "Shock-induced brittle cracking in HVPE-GaN processed by laser lift-off techniques," *J. Phys. D: Appl. Phys.* 46, 205103 (2013).
11. K. Osamura, K. Nakajima, Y. Murakami, P. H. Shingu, and A. Ohtsuki, "Fundamental absorption edge in GaN, InN and their alloys," *Solid State Commun.* 11, 617–621 (1972).
12. T. S. Kang, X. T. Wang, C. F. Lo, F. Ren, S. J. Pearton, O. Laboutin, Y. Cao, J. W. Johnson, and J. Kim, "Simulation and experimental study of ArF 193 nm laser lift-off AlGaIn/GaN high electron mobility transistors," *J. Vac. Sci. Technol. B* 30, 011203 (2012).

---

## Corresponding Author

Snehil\*

PhD Student, Kalinga University, Raipur